# 650. Effect of vacancy defect on natural vibrations of a single walled carbon nanotube as ultrahigh nanoresonators

**Ardeshir Karami Mohammadi, Mojtaba Amjadipoor**
Department of Mechanical Engineering, Islamic Azad University of Iran,
Karaj Branch, Karaj, Iran
**E-mail:** *akaramim@yahoo.com*

*(Received 12 May 2011; accepted 1 September 2011)*

**Abstract.** In this paper, the effect of vacancy defect on natural vibrations of single walled carbon nanotubes (SWCNTs) is investigated. Vacancy defect occurs during growth process therefore determining natural frequency of defected SWCNTs is very important for improving their sensing or actuating performance. Molecular dynamics and finite element methods have been employed to simulate SWCNTs. Related stiffness is calculated from molecular potential energy. Accuracy of modeling is determined by comparing our results of predicting ideal SWCNT natural frequency with the results from the previous studies. Two cases are studied. First, vacancies are scattered randomly on SWCNT structure for better simulation of actual condition, and effect of aspect ratio, vacancy ratio, and boundary conditions on natural vibration of defected SWCNTs is investigated. Second, single vacancy is considered and effect of aspect ratio, vacancy position and boundary conditions on natural vibration of defected SWCNTs is investigated. Zigzag carbon nanotubes with chirality indices (8, 0) and (10, 0) are studied in both cases. The results, in the first case, indicate that by increasing aspect ratio, the principal natural frequency shift decreases. This shift is affected by vacancy ratio. Distribution of vacancies affect natural frequency shift. As vacancies approach to the clamped end, natural frequency shift increases. In the second case, effect of aspect ratio, vacancy position, and boundary conditions is investigated.

**Keywords:** Carbon nanotube, vacancy defect, natural vibration.

## Introduction

Carbon nanotubes possess superior properties such as ultra-high strength, high electrical and thermal conductivity, high natural frequency due to their ideally perfect structures [1-3]. SWCNTs are good candidates for high-frequency actuators because of their high natural frequency. Accurate prediction of principal frequency of resonators affects their operation. Resonators are key components in signal processing systems [4]. Reduction in the size of a resonator enhances its resonant frequency and reduces its energy consumption [4]. For sensors, higher resonant frequency means higher sensitivity [5]. For wireless communications, higher frequency resonators enable the production of higher frequency filters, oscillators, and mixers [4]. CNTs have favorable properties, such as extremely high in-plane elastic modulus, high natural frequency and thermal conductivity. These properties, combined with their nanometer-sized, perfect atomic structure, imply that CNTs have potential applications in nanoelectromechanical systems, such as components for high-frequency oscillators in sensing and signal processing applications [5-7].

Use of the resonance of a cantilevered CNT have been studied by Poncharal [7]. Jensen et al. [5] demonstrated a room-temperature, CNT-based nanomechanical resonator with atomic mass resolution, based on a nanotube radio receiver design [6]. The potential of double-walled

CNTs (DWCNTs) as nanoresonators have been explored by using atomistic modeling technique [8]. Meanwhile, the defects in nanotubes, including substitutional impurities, vacancies, and topologic defects, etc. [9–12] create heterogeneous structures, which can modify electronic, chemical and mechanical properties of carbon nanotubes, and in consequence, seriously influence their applications in nanoelectromechanical systems (NEMS) and nanocomposites [12–18]. The Stone-Wales (SW) defects (namely twinned pentagon heptagon pairs [19]) and vacancies are typical defects observed in carbon nanotubes. For example, it was suggested that 2%–5% carbon atoms are involved in SW defective sites [20]. Zhou et al. investigated the transport properties of defected zigzag metallic single-walled nanotubes (SWNTs) [21] and found that the circumferential interference dependent on the defect configuration is responsible for the transport blocking observed experimentally [22]. Tunvir et al. studied the mechanical properties of SWNTs having two neighboring vacancy defects or SW defects, and revealed that the defect configuration in the SWNT structure is one of the key factors in determining its mechanical properties, as well as the population of defects [23]. Barinov et al. [24] and Kim et al. [25] studied the adsorption and transport of metallic atoms on multi-walled carbon nanotubes (MWNTs). The diffusion mechanism of indium atoms along MWNTs was revealed by means of photoemission spectromicroscopy and density functional theory calculations: the indium transport is controlled by the concentration of defects in the C network and proceeds via hopping of indium atoms between C vacancies [24]. The calculations of Pt nanoparticles loaded on the defective carbon nanotubes showed that the adsorption of Pt atom on the vacancy of nanotube was significantly stronger by s-p hybridization with carbon atoms near the defect site [25]. It is well believed that the defect configurations may seriously influence the mechanical and electrical properties of carbon nanotubes.

In this paper, the effect of vacancy defects on natural vibration of single walled carbon nanotubes is investigated. Vacancy defects occur during growth process so determining natural frequency of defected SWCNTs is very important for improving their actuating performance. Molecular dynamics and finite element methods have been employed to simulate SWCNTs. Related stiffness is calculated from molecular potential energy. Two cases are studied. First, vacancies are scattered randomly on SWCNT structure for better simulation of actual condition, and effect of aspect ratio, vacancy ratio, and boundary conditions on natural vibration of defected SWCNTs is investigated. Second, single vacancy is considered and effect of aspect ratio, vacancy position and boundary conditions on natural vibration of defected SWCNTs is investigated. Zigzag carbon nanotubes with chirality indices (8, 0) and (10, 0) are studied in both cases.

## Modeling

Molecular dynamics method has been used for simulations. The basic premise in this method is that CNT can be modeled as a continuum having continuous distributions of mass and stiffness. Odegard [26] used an equivalent continuum model for prediction of structural property of nanostructure materials. Bending rigidity of graphene sheet was determined based on this method [27]. Extensional, torsional and bending rigidity of SWNTs was determined using the potential energy for the inter-atomic forces of a molecular mechanics model [28]. Li & Chou [3, 29] developed a similar method using continuum mechanics and molecular dynamics for predicting static and dynamic properties of CNTs. Thus we can simulate a SWCNT as a space frame consisting of mass and stiffness. The most part of atom mass is related to nucleus so nucleus mass ($m_c = 1.9943 \times 10^{-26}\ Kg$) is considered as atom mass and Electron masses are neglected. Mass element is located on carbon atom position in CNT

structure for simulation of atoms mass. Bonding of carbon atoms is modeled by linear elastic stiffness element. Fig. 1 shows the inter-atomic interactions modeled with this approach.

Total stretching potential energy was expressed as sum of energies due to valance or bonded interactions and non-bonded interactions [31].

$$U = \sum U_r + \sum U_\theta + \sum (U_\varphi + U_\omega) + \sum U_{vdW} \quad (1)$$

where $U_r$, $U_\theta$, $U_\varphi$, $U_\omega$ and $U_{vdW}$ are the energy terms due to bond stretching, bond angle bending, dihedral angle torsion, out-of-plane torsion and van der Waals interactions, respectively.

In this research, the term related to van der Waals interaction has been ignored. So Equation 1 can be expressed as:

$$U = \sum U_r + \sum U_\theta + \sum (U_\varphi + U_\omega) \quad (2)$$

where:

$$U_r = \sum_{bonds} k_r (r - r_{eq})^2 \quad (3)$$

where $k_r$ is the bond stretching force constant, r the distance and $r_{eq}$ the equilibrium distance between atoms.

$$U_\theta = \sum_{angles} k_\theta (\theta - \theta_{eq})^2 \quad (4)$$

where $k_\theta$ is the bond-angle bending force constant, $\theta$ the bond-angle, and $\theta_{eq}$ the equilibrium bond-angle.

$$U_\varphi + U_\omega = \sum_{dihedral} k_\tau (\varphi - \varphi_{eq})^2 \quad (5)$$

where $k_\tau$ is torsional resistance constant, $\varphi$ the torsion angle, and $\varphi_{eq}$ the equilibrium torsion angle.

From structural mechanics viewpoint, potential energy for elastic element can be expressed as:

$$U = \frac{1}{2} k [\Delta r)]^2 \quad (6)$$

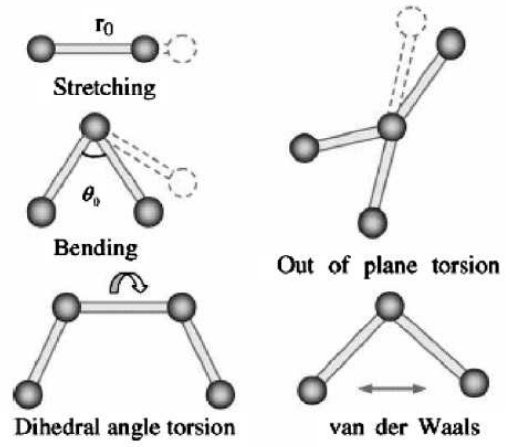


**Fig. 1.** Inter-atomic interactions

Therefore, related molecular potential energy can be simulated similarly to mechanical element potential energy, and considering equivalence of the energies, force filed space frame model is created. To simulate the vacancy defects, the related elements were omitted in the frame like model. The force constant values are chosen based upon the experience with graphite sheets: $\frac{k_r}{2} = 469\ kcal\ mol^{-1}\ A^{0\ (-2)}$, $\frac{k_\theta}{2} = 63\ Kcal\ mol^{-1}rad^{-2}$. The force constant $k_\tau$ is adopted as $\frac{k_\tau}{2} = 20\ Kcal\ mol^{-1}rad^{-2}$ based on Cornell results [32]. The capability and efficiency of this molecular structural mechanics method have been verified in the modeling of single walled carbon nanotubes under tension or torsion. The calculated results of Young's modulus and shear modulus are in good agreement with the theoretical predictions and experimental results available in the literature [29].

**Analysis method**

For the free vibration of undamped structure problem, the equation of motion is:

$$[M]\{\ddot{y}\} + [K]\{y\} = 0 \tag{7}$$

where $[M]$ and $[K]$ are the global mass and stiffness matrices, respectively, and $\{y\}$ and $\{\ddot{y}\}$ are nodal displacement and acceleration vectors, respectively. The global stiffness matrix of the frame structure can be assembled from the elemental stiffness matrices: $[K] = \sum_{e=1}^{n} [K]^e$, where n is the number of elements. For assembling nodes, finite element method was used. According to the model, $[K]^e$ can be expressed as:

$$[K]^e = \begin{bmatrix} [k_{ii}] & [k_{ij}] \\ [k_{ji}] & [k_{jj}] \end{bmatrix} \tag{8}$$

where submatrices $[k_{ii}]$, $[k_{ij}]$, $[k_{ji}]$ and $[k_{jj}]$ express the related stiffness of element i-j.

The global mass matrix $[M]$ can be obtained from elemental mass matrix.

The coefficients in the mass matrix corresponding to flexural rotation and torsional rotation are assumed to be zero. Only the coefficient corresponding to translator displacements are kept. Thus the elemental mass matrix is expressed as:

$$[M]^e = diag\left[\frac{m_c}{3}\ \frac{m_c}{3}\ \frac{m_c}{3}\ 0\ 0\ 0\right] \tag{9}$$

The factor is introduced because of the three bonds of carbon atom connecting with the three nearest neighboring atoms. The natural frequencies $f$ and mode shapes are determined from the solution of the eigenproblem

$$([K]_s - \omega^2[M]_s)\{y_0\} = 0 \tag{10}$$

where $[K]_s$ and $[M]_s$ are the condensed stiffness and mass matrices, respectively, $\{y_0\}$ is the displacement vector, and $\omega = 2\pi f$ is the angular frequency.

**Results and discussion**

For validation of our modeling technique, the results were compared with those from Li and Chou [3] (Fig. 2). Perfect SWCNT with chirality index (8, 0) and bridged boundary condition

was considered. As Fig. 2 indicates our results are close to those of Li and Chou. Fig. 3 illustrates some mode shapes of the SWCNTs.

To investigate the effect of vacancy defect on natural frequency of SWCNTs, two cases are considered:

**Case 1.** In this case, vacancies are created randomly on CNTs structure with different ratios. So vacancy ratio $\frac{n_1}{n} \times 100$ has been defined to express the percentage of vacancies. Where *n* refers to number of total nodes in CNT's structure, and $n_1$ is number of nodes which have been vanished as vacancies. Creation of random vacancies has been performed under two limitations. First, two neighboring nodes can not be eliminated together. Second, vacancies should be distributed uniformly.

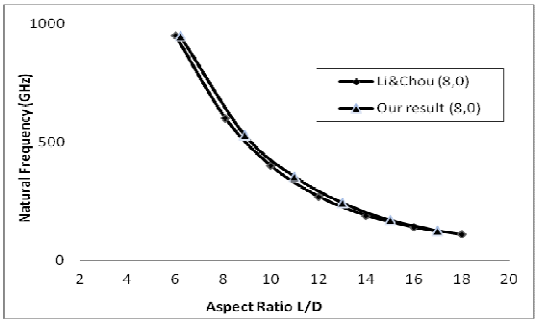


**Fig. 2.** Results for perfect SWCNT with chirality index (8, 0) and bridged boundary condition compared with results obtained by Li and Chou

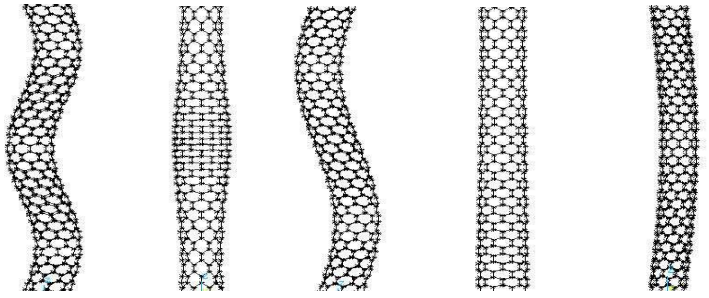

**Fig. 3.** Some SWCNTs mode shapes

Fig. 4 shows the natural frequency shift of SWCNT with chirality index (8, 0). Cantilevered boundary condition with different aspect ratio and different vacancy ratios has been considered. As Fig. 4 indicates, SWCNT with vacancy ratio equal to 2% and aspect ratio of 5 has natural frequency that is approximately 80 GHz less than for the case of perfect one. So vacancies affect the principal natural frequency of nanotubes considerably. It is evident from Fig. 4 that as vacancy ratio increases, the frequency increases as well. When vacancy ratio percent is equal or more than 1.17, the slope of diagram increases, therefore, the effect of vacancies on the frequency increases.

Fig. 5 demonstrate the natural frequency shift of SWCNT with chirality index (8, 0). Bridged boundary condition with different aspect ratio and different vacancy ratios has been considered. Fig. 5 indicates, for SWCNT, when vacancy ratio is 1.88 and aspect ratio is 5, the natural frequency shift is equal to 126 GHz. Fig. 5 reveals that relation between diameter and

length and frequency shift is the same as in Fig. 4. Comparison of Fig. 4 and Fig. 5 leads to conclusion that boundary condition affects the effect of vacancy defect on principal frequency of SWCNTs. Natural frequency shift in bridged boundary condition is more than in the case of cantilevered one.

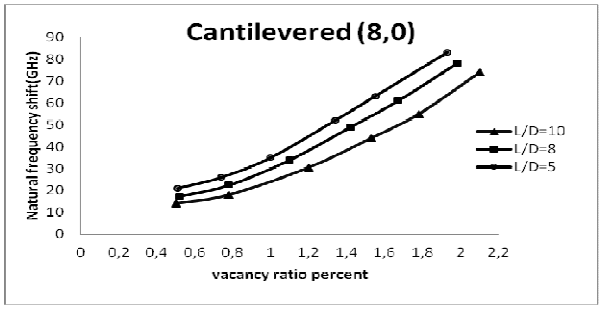


**Fig. 4.** Shift of principal natural frequency of cantilevered SWCNT, with chirality (8, 0)

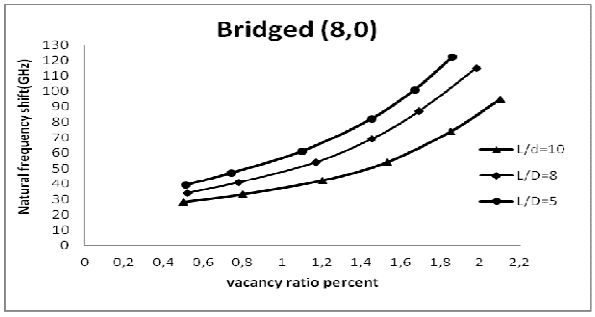


**Fig. 5.** Shift of principal natural frequency of bridged SWCNT, with chirality index (8, 0)

Fig. 6 shows the natural frequency shift of SWCNT with chirality index (10, 0). Cantilevered boundary condition with different aspect ratio and different vacancy ratios has been considered. As Fig. 6 indicates SWCNT with vacancy ratio equal to 2.1% and aspect ratio of 7 has natural frequency approximately 38 GHz less than for the case of perfect one. It is evident from Fig. 6 that the natural frequency shift decreases with increase in aspect ratio.

Fig. 7 illustrates natural frequency shift of SWCNT with chirality index (10, 0). Bridged boundary condition with different aspect ratio and different vacancy ratios has been considered. As Fig. 7 indicates SWCNT with vacancy ratio equal to 2.1% and aspect ratio equal to 7 has natural frequency approximately 54 GHz less than for the case of perfect one. Fig. 7 reveals that natural frequency shift decreases when aspect ratio increases. When vacancy ratio is equal to or more than 0.9, the effect of vacancy is increased. Comparison of Fig. 6 and Fig. 7 leads to the conclusion that boundary condition influences the effect of vacancy defect on principal frequency of SWCNTs. Natural frequency shift in bridged boundary condition is more pronounced with respect to the case of the cantilevered one.

**Case 2.** In this case, single vacancy is considered, and effect of aspect ratio, vacancy position, and boundary conditions on natural frequency shift of defected SWCNTs compared to undefected SWCNTs is investigated. So vacancy position $X/L$ has been defined to express the nondimensional position of a vacancy, where X is vacancy position and $L$ is the length of nano tube. Fig. 8 shows the natural frequency shift of SWCNT with chirality index (8, 0). Cantilevered boundary condition with different aspect ratio and different vacancy positions has been considered. Fig. 8 reveals that as vacancy approaches to the clamped end, natural frequency shift increases. SWCNT with vacancy position near to 0.7 and aspect ratio equal to 5,

natural frequency shift is ignorable and for vacancy position greater than 0.7, the shift is reversed.

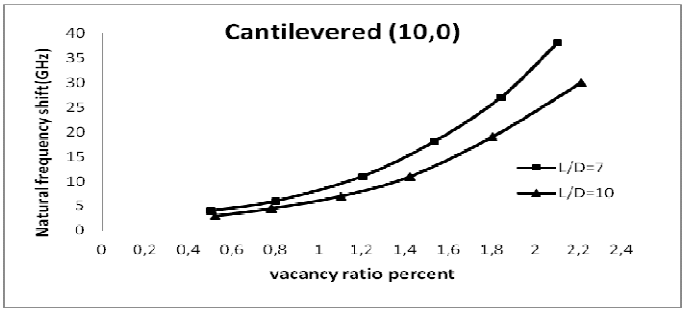


**Fig. 6.** Shift of principal natural frequency of cantilevered SWCNT, with chirality (10, 0)

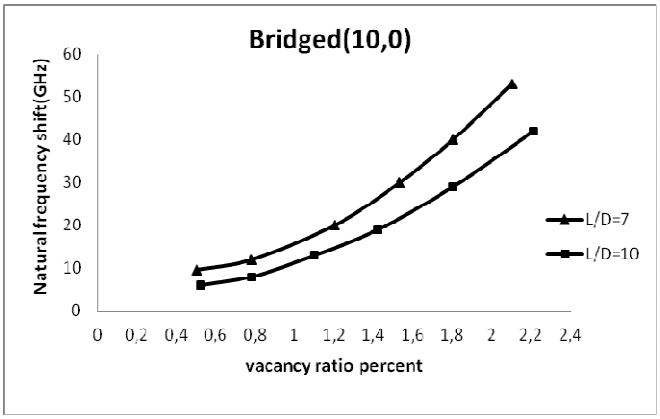


**Fig. 7.** Shift of principal natural frequency of bridged SWCNT, with chirality index (10, 0)

Fig. 9 provides natural frequency shift of SWCNT with chirality index (8, 0). Bridged boundary condition with different aspect ratio and different vacancy positions has been considered.

Figs. 10 and 11 provide natural frequency shift of SWCNT with chirality index (10, 0). Cantilevered boundary condition and bridged boundary condition, respectively, with different aspect ratio and different vacancy positions has been considered.

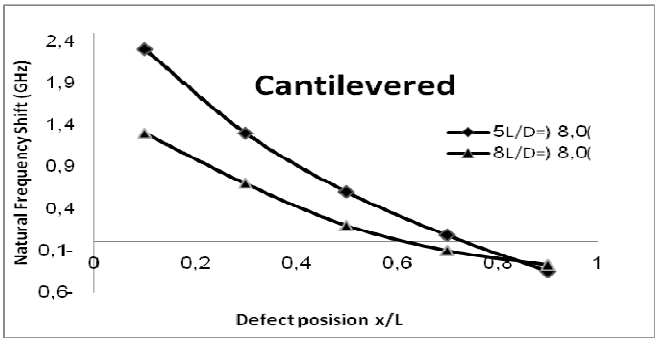


**Fig. 8.** Shift of principal natural frequency of cantilevered SWCNT, with chirality (8, 0)

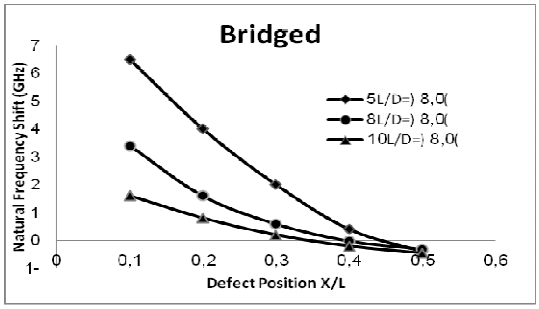


**Fig. 9.** Shift of principal natural frequency of bridged SWCNT, with chirality index (8, 0)

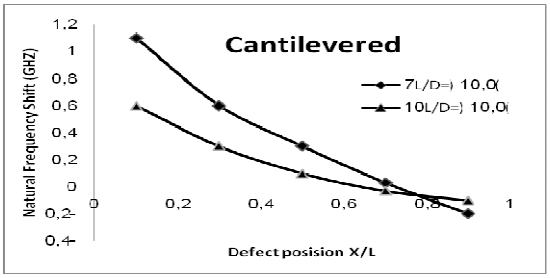


**Fig. 10.** Shift of principal natural frequency of cantilevered SWCNT, with chirality (10, 0)

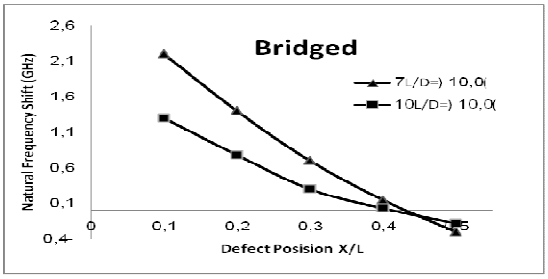


**Fig. 11.** Shift of principal natural frequency of bridged SWCNT, with chirality index (10, 0)

## References

**[1]** **Treacy M. M. J., Ebbesen T. W., Gibson J. M.** Exceptionally high Young's modulus observed for individual carbon nanotubes. Nature, 1996, 381, p. 678–680.

**[2]** **Ebbesen T. W., Lezec H. J., Hiura H., et al.** Electrical conductivity of individual carbon nanotubes. Nature, 1996, 382, p. 54–56.

**[3]** **Li C., Chou T.-W.** Single-walled nanotubes as ultrahigh frequency nanomechanical resonators. Phys. Rev. B 2003; 68, 073405.

**[4]** **De Los Santos H. J.** Introduction to Microelectromechanical Microwave Systems. Artech House Publishers, London, 1999.

**[5]** **Jensen K., Kim K., Zettl A.** Nature Nanotechnology, 3 (2008), p. 533.

**[6]** **Jensen K., Weldon J., Garcia H., Zettl A.** Nano Lett., 7 (2007), 3508.

**[7]** **Poncharal P., Wang Z. L., Ugarte D., De Heer W. A.** Science 283 (1999), 1513.

**[8]** **Jeong Won Kanga, Oh Kuen Kwonb, Jun Ha Lee, Young Gyu Choi, Ho Jung Hwang** Frequency change by inter-walled length difference of double-wall carbon nanotube resonator. Solid State Communications, 149 (2009) p. 1574–1577.

**[9]** **Dunlap B. I.** Connecting carbon tubules. Phys. Rev. B, 1992, 46, p. 1933–1936.

**[10]** **Banhart F.** Irradiation effects in carbon nanostructures. Rep. Prog. Phys., 1999, 62, p. 1181–1221.

**[11] Choi H. J., Ihm J., Louie S. G., et al.** Defects, quasibound states, and quantum conductance in metallic carbon nanotubes. Phys. Rev. Lett., 2000, 84, p. 2917–2920.
**[12] Suenaga K., Wakabayashi H., Koshino M., et al.** Imaging active topological defects in carbon nanotubes. Nature, 2007, 2, p. 358–360.
**[13] Alexandre S. S., Mazzoni M. S. C., Chacham H.** Edge states and magnetism in carbon nanotubes with line defects. Phys. Rev. Lett., 2008, 100: 146801.
**[14] Qian D., Wagner G. J., Liu W. K., et al.** Mechanics of carbon nanotubes. Appl. Mech. Rev., 2002, 55, p. 495–533.
**[15] Srivastava D., Menon M., Cho K.** Computational nanotechnology with carbon nanotubes and fullerenes. Comput. Sci. Eng., 2001, 3, p. 42–55.
**[16] Wang C. C., Zhou G., Wu J., et al.** Effects of vacancy-carboxyl pair functionalization on electronic properties of carbon nanotubes. Appl. Phys. Lett., 2006, 89: 173130.
**[17] Wang C. C., Zhou G., Liu H. T., et al.** Chemical functionalization of carbon nanotubes by carboxyl groups on Stone-Wales defects: A density functional theory study. J. Phys. Chem. B, 2006, 110, p. 10266–10271.
**[18] Park J. Y.** Electrically tunable defects in metallic single-walled carbon nanotubes. Appl. Phys. Lett., 2007, 90: 023112.
**[19] Stone A. J., Wales D. J.** Theoretical studies of icosahedral C60 and some related species. Chem. Phys. Lett., 1986, 128, p. 501–503.
**[20] Monthioux M.** Filling single-wall carbon nanotubes. Carbon, 2002, 40, p. 1809–1823.
**[21] Zhou T., Wu J., Duan W. H., et al.** Physical mechanism of transport blocking in metallic zigzag carbon nanotubes. Phys. Rev. B, 2007, 75: 205410.
**[22] Gómez-Navarro C., De Pablo P. J., Gómez-Herrero J., et al.** Tuning the conductance of single-walled carbon nanotubes by ion irradiation in the Anderson localization regime. Nat. Mat., 2005, 4, p. 534–539.
**[23] Tunvir K., Kim A., Nahm S. H.** The effect of two neighboring defects on the mechanical properties of carbon nanotubes. Nanotechnology, 2008, 19: 065703.
**[24] Barinov A., Üstünel H., Fabris S., et al.** Defect-controlled transport properties of metallic atoms along carbon nanotube surfaces. Phys. Rev. Lett., 2007, 99: 046803.
**[25] Kim S. J., Park Y. J., Ra E. J., et al.** Defect-induced loading of Pt nanoparticles on carbon nanotubes. Appl. Phys. Lett., 2007, 90: 023114.
**[26] Odegard G. M., Gates T. S., Nicholson L. M., Wise K. E.** Equivalent continuum modeling of nano-structured materials. Compos. Sci. Technol., 2002; 62: p. 1869–80.
**[27] Gates T. S., Odegard G. M., Frankland S. J. V., Clancy T. C.** Computational materials: multi-scale modeling and simulation of nanostructured materials. Compos. Sci. Technol., 2005; 65(15-16): p. 2416–34.
**[28] Bodily B. H., Sun C. T.** Structural and equivalent continuum properties of single-walled carbon nanotubes. Int. J. Mater. Product. Technol., 2003; 18(4/5/6): p. 381–97.
**[29] Li C., Chou T.-W.** A structural mechanics approach for the analysis of carbon nanotubes. Int. J. Solids Struct., 2003; 40: p. 2487–99.
**[30] Ronald F. Gibson, Emmanuel O. Ayorinde, Yuan-Feng Wen.** Vibration of carbon nanotubes and their composites: A Review. Composite Science, 2007.
**[31] Rappe A. K.** J. Am. Chem. Soc., 114, 10024, 1992.
**[32] Cornell W. D., Cieplak P., et al.** Journal of the American Chemical Society, 117, (1995), 5179.